Journal of Applied Electrochemistry **34**: 469–476, 2004.

Design and modelling of a dialysis membrane electrochemical reactor (D-MER) for oxidoreductase-catalysed synthesis

K. DÉLÉCOULS-SERVAT[1], A. BERGEL[2] and R. BASSEGUY[2,*]
[1]*Present address: Laboratoire de Catalyse en Chimie Organique (Equipe Electrocatalyse) – UMR 6503 CNRS, Université de Poitiers, 40 avenue du Recteur Pineau, 86022 Poitiers, Cedex, France*
[2]*Laboratoire de Génie Chimique – CNRS UMR 5503, Basso Cambo, 5 rue Paulin Talabot, BP 1301, 31 106 Toulouse, France*
*(*author for correspondence, fax: +33 5 34615253, e-mail: Regine.Basseguy@ensiacet.fr)*

Received 15 July 2003; accepted in revised form 2 December 2003

Key words: electrochemistry, enzyme, filter-press reactor, membranes, reaction engineering, synthesis

Abstract

The study is the first step in a design of an electrochemical reactor able to process enzyme catalysed electrochemical synthesis. To develop economically efficient synthesis, the enzymes must be confined very close to the electrode surface. Here, the confinement was achieved with a dialysis membrane integrated in a classic filter-press electrochemical reactor. A simple electrochemical reaction, without enzymatic catalysis, was used to model the behaviour of the 'dialysis membrane electrochemical reactor' (D-MER). The values of the physicochemical parameters were determined by independent experiments, and the thickness of the reaction layer in the reactor was the only parameter to be adjusted numerically. The conditions of this adjustment were discussed. The model gave a good fit to the experimental data and consequently proved that the current design of the reactor is ready to be used with more complex reactions as enzymatic synthesis. A first example was described, based on the glucose oxidase-catalysed synthesis of gluconic acid.

List of symbols

A electrode surface area (m^2)
C concentration (M)
d membrane thickness (m)
D diffusion coefficient ($m^2\ s^{-1}$)
E potential (V vs SCE)
E'° normal apparent potential (V vs SCE)
F faradaic constant ($C\ mol^{-1}$)
I current (A)
n number of exchanged electrons
T temperature (K)
x distance from the electrode surface (mm)

Subscripts
l reaction layer
lim diffusion-limited
m membrane
red reduced species
ox oxidized species

Greek letters
δ reaction layer thickness (m)
ν viscosity ($m^2\ s^{-1}$)
ω angular velocity ($rad\ s^{-1}$)

1. Introduction

A bioelectrochemical process consists in the association of biochemical reactions with an electrochemical system. The aim is to optimally exploit the high selectivity of biochemical reactions to design clean and efficient syntheses [1]. One of the first reactors coupling enzymatic catalysis and electrochemistry was proposed by Whitesides [2, 3], and later by Maeda and Kajiwara [4]. In both cases, the enzymes were free in solution or immobilized as a soluble suspension. However, only the enzyme near the electrode surface was really effective. Most of the enzyme in the bulk was too far from the electrode surface to be involved in the process. Consequently, economically efficient reactors require the enzymes to be confined in the strict vicinity of the electrode surface. The methods cited in the literature to immobilize and confine the enzyme can be classified by technique into two types: chemical and physical. For the first type, methods such as covalent attachment [5] or the use of enzyme crosslinked crystals [6] have revealed high efficiency compared with soluble enzyme. Physical methods include adsorption, entrapment in a film or confinement with a membrane. These different methods (used alone or combined) have been compared by Miyawaki and Yano [7], and more recently by Bartlett et al. [8]. In the present investigation we have chosen to

retain the enzyme in the strict vicinity of the electrode with a semipermeable membrane.

Numerous examples of enzymatic membrane reactors already exist where no electrochemical step intervenes. Two types can be distinguished: those using a dialysis membrane often called membrane enclosed enzymatic catalysis (MEEC) [9] and those with a filtration membrane. In this last case, authors proposed to use different kinds of membranes: filtration membranes simultaneously weighing down the compounds that must be retained [10], nanofiltration membranes [11], hydrophobic microfiltration membranes [12], and also charged filtration membranes, which retain the compounds combining effects of size exclusion and electrostatic repulsion [13, 14]. These studies only dealt with membrane reactors that did not involve an electrochemical step.

In the case of a coupled electrochemical/membrane system, two different set-ups are found in the literature: split and compact configurations. In the split system, the electrochemical and membrane reactors are two separate apparatuses incorporated in a solution loop. The membrane reactor removes the product continuously and keeps the enzyme in the loop [15–17]. In the compact configuration, the electrochemical and enzymatic reactors are integrated in the same apparatus. A theoretical study showed that the performance is higher with a compact process. In this the electrochemical and enzymatic reactions occur in the same apparatus rather than in two different reactors [18]. Nevertheless, only one example of a compact reactor has been proposed [19]. This reactor was only a first experimental attempt, the working electrode being simply inserted into a dialysis tubing, but gave very promising results: almost complete transformation (95%) was obtained in 8 days for the synthesis of L-lactate with an enantiomeric purity superior to 98%. This process would surely benefit from a better design. The purpose of this work is to develop the same general approach by integrating the dialysis confinement membrane into a classical filter-press electrochemical reactor.

The advantages of a compact reactor compared to a split one should be underlined. In a compact equipment the enzyme is confined in a small volume, called the reaction layer, near the electrode surface. This allows the use of a minimal quantity of enzyme for a maximal volume of solution to be processed. Also, the enzyme is in solution, and its structure and activity are consequently not affected. The whole quantity of enzyme that is put in the reactor is effective, there is no loss, as is the case with most immobilisation techniques. Moreover, confined near the electrode, the enzyme does not circulate in the pump or the pipes of the external loop. Denaturing phenomena such as adsorption on the walls are consequently avoided. In addition, when a reaction requires anaerobic conditions, nitrogen bubbling is often used in the storage tank to eliminate oxygen. The occurrence of gas–liquid interfaces is a strong denaturing factor for enzymes. In a compact reactor, nitrogen bubbling in the storage tank is no longer a problem since the enzyme, confined near the electrode, is not present in the storage tank. Sometimes using a compact reactor is essential, for example, for the transformation of glucose into gluconic acid catalysed by a glucose oxidase (GOD):

$$C_6H_{12}O_6 + O_2 + H_2O \xrightarrow{GOD} C_6H_{12}O_7 + H_2O_2 \qquad \text{(Reaction 1)}$$

This reaction produces hydrogen peroxide, which strongly inhibits GOD. Hydrogen peroxide can be easily eliminated via its electrochemical oxidation into oxygen:

$$H_2O_2 \longrightarrow O_2 + 2H^+ + 2e^- \qquad \text{(Reaction 2)}$$

Nevertheless, if GOD is in bulk far from the electrode surface, hydrogen peroxide can inhibit the enzyme before it reaches the electrode surface to be eliminated. In contrast in a compact membrane electrochemical reactor the enzyme is confined close to the electrode surface and hydrogen peroxide is produced only in the strict vicinity of the electrode, and is consequently oxidized immediately. Therefore, the inhibition of GOD by hydrogen peroxide should be avoided or drastically reduced.

The aim of this work was to design a compact membrane electrochemical reactor for applications involving enzyme-based synthesis. The reactor, which uses a dialysis membrane to confine the enzyme, was called a 'dialysis-membrane electrochemical reactor' (D-MER). A simple electrochemical reaction (without enzymatic catalysis) was used to validate and improve the concept. A model for the D-MER behaviour was proposed and the values of the required parameters were determined with independent experiments. The D-MER was applied to the production of gluconic acid from glucose catalysed by GOD. A range of 0.25–0.3 M for the concentration of glucose was deliberately chosen here with the aim of approaching conditions used in the industrial production of gluconic acid by fermentation [20, 21].

2. D-MER: description and procedures

2.1. *Reactor description*

The principle of the reactor is to confine the enzyme in solution, near the electrode, by means of a dialysis membrane. The D-MER shown in Figure 1 was a filter-press reactor made of three Plexiglass pieces of 26 cm × 13 cm (4,7,8). The working electrode (2) and the auxiliary electrode (1) were platinum grids (15 cm × 2 cm). Electrical connections of the working and auxiliary electrodes were made with platinum wire (14 and 15). The saturated calomel reference electrode (13), was connected to the reactor with a Luggin

capillary (12). The working electrode was covered by a dialysis membrane (11) (molecular weight cut off 12–14 kDa). The enzyme was introduced behind the membrane thanks to a capillary (16). When necessary a Nafion® membrane (3) could be inserted to separate the working and auxiliary compartments. This last membrane ensures ionic conduction and avoids any transfer of reactant or product between the two compartments. With or without a Nafion® membrane, the solution(s) circulated in a loop, including the reactor, a pump (5,10) and a 150 cm^3 storage tank (6,9). When anaerobic conditions are required a flux of inert gas (argon or nitrogen) can be sent through the storage tank. In all cases, the solution circulated tangentially with respect to the dialysis membrane.

The working compartment is divided into three zones schematized in Figure 1:

(i) $0 < x < \delta$: the reaction layer, where the enzyme is confined in solution near the electrode surface;
(ii) $\delta < x < \delta + d$: the membrane, which confines the enzyme;
(iii) $x > \delta + d$: the bulk, which is considered as well stirred.

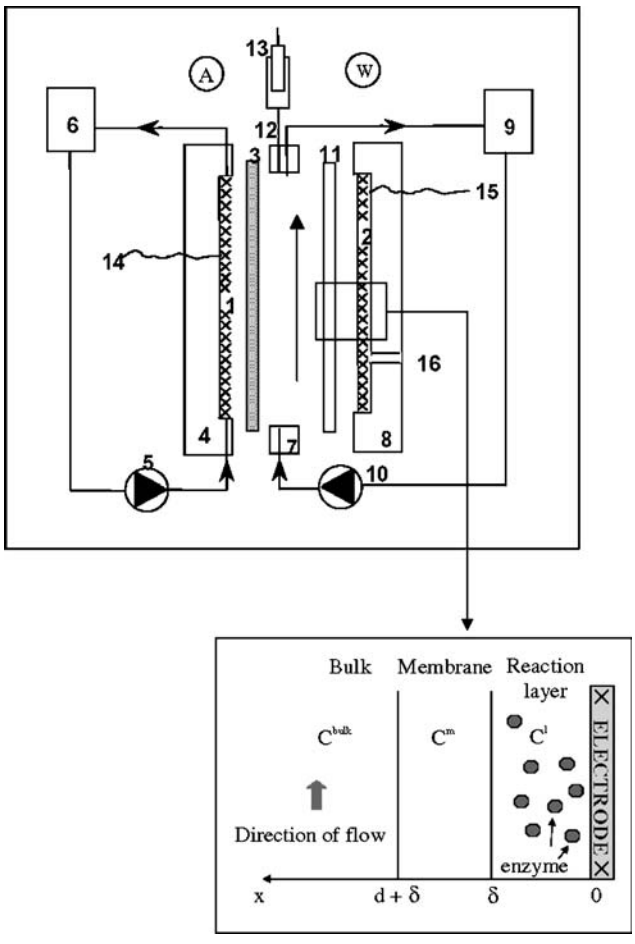

Fig. 1. Schematic representation of the dialysis-membrane electrochemical reactor (D-MER). (1) auxiliary electrode, (2) working electrode, (3) Nafion® membrane, (4,7,8) plexiglass pieces, (6,9) storage tank, (5,10) pump, (11) dialysis membrane, (12) Luggin capillary, (13) reference electrode, (14,15) platinum wire, (16) capillary for the reaction layer filling.

2.2. *Procedures*

To optimize the reactor design, a simple electrochemical system, without enzymatic catalysis, was used (Reaction 3). The standard experiments consisted in recording voltammograms in solution containing hexacyanoferrate (III).

$$Fe(CN)_6^{3-} + 1e^- \leftrightarrow Fe(CN)_6^{4-} \qquad \text{(Reaction 3)}$$

3. Theory

A numerical model was developed to simulate the electrochemical kinetics and mass transfers in the D-MER for a simple electrochemical reaction: Ox + - $ne^- \leftrightarrow$ Red.

The transient mass balance equations were written for the zones described in Figure 1. The diffusion coefficients of oxidized and reduced species were assumed to be equal.

In the reaction layer ($0 < x < \delta$)

$$\frac{\partial C_{ox}}{\partial t} = D_l \frac{\partial^2 C_{ox}}{\partial x^2} \tag{1}$$

and

$$\frac{\partial C_{red}}{\partial t} = D_l \frac{\partial^2 C_{red}}{\partial x^2} \tag{2}$$

In the membrane ($\delta < x < \delta + d$)

$$\frac{\partial C_{ox}}{\partial t} = D_m \frac{\partial^2 C_{ox}}{\partial x^2} \tag{3}$$

and

$$\frac{\partial C_{red}}{\partial t} = D_m \frac{\partial^2 C_{red}}{\partial x^2} \tag{4}$$

At the membrane–solution interface ($x = d + \delta$), the concentrations of the oxidized and reduced species were equal to the concentrations in the bulk, which is assumed to be well stirred:

$$C_{ox}|_{x=d+\delta} = C_{ox}^{bulk} \tag{5}$$

and

$$C_{red}|_{x=d+\delta} = 0 \tag{6}$$

At the reaction layer–membrane interface ($x = \delta$), the flux of each species was equal on both sides:

$$D_m \left.\frac{\partial C_{ox}}{\partial x}\right|_{x=\delta^+} = D_l \left.\frac{\partial C_{ox}}{\partial x}\right|_{x=\delta^-} \quad (7)$$

$$D_m \left.\frac{\partial C_{red}}{\partial x}\right|_{x=\delta^+} = D_l \left.\frac{\partial C_{red}}{\partial x}\right|_{x=\delta^-} \quad (8)$$

At the electrode surface ($x = 0$), the concentrations were controlled by the electrochemical conditions. When potential was applied, the electrochemical kinetics were assumed to be fast enough with respect to mass transfer and to the potential scan rate. In these conditions the concentration ratio of the oxidized and reduced species was given by the Nernst equation:

$$\frac{C_{ox}}{C_{red}} = \exp\left[\frac{nF}{RT}(E - E'^{\circ})\right] \quad (9)$$

At the electrode surface, the fluxes of oxidized and reduced species were opposite:

$$D_l \left.\frac{\partial C_{ox}}{\partial x}\right|_{x=0} = -D_l \left.\frac{\partial C_{red}}{\partial x}\right|_{x=0} \quad (10)$$

The current was calculated from the concentration gradient at the electrode surface according to

$$I = nFAD_l \left.\frac{\partial C_{ox}}{\partial x}\right|_{x=0} \quad (11)$$

All these equations and the boundary conditions were discretized according to an implicit Crank and Nicholson scheme [22]. The space step and time step values were chosen small enough not to affect the numerical results.

4. Materials and methods

4.1. *Materials*

Chemicals and glucose oxidase (GOD, E.C. 1.1.3.4) from *Aspergillus niger* were purchased from Sigma. GOD activity, which is defined as the number of micromoles of β-D-glucose consumed in one minute at pH 5.1 at 35 °C, was measured spectrophotometrically according to Sigma protocol. A Sigma diagnostic kit HK was used to spectrophotometrically measure the concentrations of glucose during the electrolysis [23]. Solutions of hexacyanoferrate(III) and glucose were prepared in 0.1 M phosphate buffer pH 7.0. The regenerated cellulose dialysis membrane was supplied by the Bioblock company. A cut-off value of 12–14 kDa was selected. Before use, the membrane was immersed in 0.1 M phosphate buffer pH 7.0 for at least 24 h. The working and auxiliary platinum grid electrodes (196 mesh cm^{-2}) were purchased from Engelhard-CLAL (France).

4.2. *Electrochemical measurements*

Cyclic voltammetry was performed with an electrochemical interface (1286 Solartron Schlumberger) monitored by a computer. All potentials were monitored and measured versus a saturated calomel electrode (SCE). The diffusion coefficients were determined in independent experiments with a platinum rotating disc electrode of 4 mm diameter (Tacussel, mod. EDI).

5. Results

5.1. *Preliminary determination of parameter values*

The membrane thickness (d), the diffusion coefficients of hexacyanoferrate(III) in solution (D_l) and in the membrane (D_m) were determined in independent experiments. The diffusion coefficients of hexacyanoferrate(II) were taken as equal to those of hexacyanoferrate(III). These values were then introduced into the model.

The diffusion coefficient of hexacyanoferrate(III) in solution was determined by reduction on a rotating platinum disc electrode. It was calculated via the Levich equation [24] and was equal to $1.32 \pm 0.04 \times 10^{-9}$ m^2 s^{-1}.

The thickness of the dry and wet membrane was determined with an electronic Palmer. The dry membrane thickness was in the range of 20–24 μm. The thickness of the wet membrane proved to be difficult to estimate. However, the average values obtained from a series of measurements led to the conclusion that multiplying the dry membrane thickness by a factor of two gave a correct estimation of the wet membrane thickness. The value used was 46 μm for the wet membrane.

For the determination of the diffusion coefficient of hexacyanoferrate(III) in the membrane, the membrane was carefully positioned against the surface of a rotating platinum disc electrode using a toric gasket. In this case, the diffusion-limited current I_{lim} was given by the equation [25, 26]:

$$\frac{1}{I_{lim}} = \frac{1}{nFAD_m \left.\frac{\partial C_{ox}}{\partial x}\right|_{x=0}} + \frac{1}{0.620\, nFD^{2/3}\omega^{1/2}\nu^{-1/6}(C_{ox}^{bulk} - C_{ox}^{int})} \quad (12)$$

where C_{ox}^{int} is the concentration of the oxidized species at the bulk solution–membrane interface.

This equation can be simplified when the resistance due to diffusion in solution becomes negligible with respect to the resistance due to diffusion in the membrane. This corresponds to a high angular velocity:

$$\frac{1}{I_{lim}} = \frac{1}{nFAD_m \left.\frac{\partial C_{ox}}{\partial x}\right|_{x=0}} \quad (13)$$

Table 1. Value of the different parameters used in the model

Parameter	Value
Initial concentration of hexacyanoferrate(III)	10 mM
Initial concentration of hexacyanoferrate(II)	0 mM
Dialysis membrane thickness (12–14 kDa)	46 μm
Exchanged electron number for hexacyanoferrate(III) reduction	1
Diffusion coefficient of hexacyanoferrate(III) and hexacyanoferrate(II) in solution	1.3×10^{-9} m^2 s^{-1}
Diffusion coefficient of hexacyanoferrate(III) and hexacyanoferrate(II) in membrane 12–14 kDa	1.6×10^{-10} m^2 s^{-1}
Standard potential of hexacyanoferrate(III) and hexacyanoferrate(II)	0.195 V vs SCE

By expressing the concentration gradient in the membrane, the transfer coefficient can be determined by:

$$\frac{D_m}{d} = \frac{I_{lim}}{nFAC_{ox}^{bulk}} \tag{14}$$

The diffusion-limited current increased up to angular velocity of 47 rad s^{-1}. It stabilised for higher values, the maximal diffusion limiting current being equal to 4.36×10^{-5} A with C_{ox}^{bulk} equal to 10 mM. The transfer coefficient and the apparent diffusion coefficient (D_m) can be derived from the following values:

$$\left(\frac{D_m}{d}\right) = 3.6 \times 10^{-6}\,\text{m s}^{-1} \text{ gave } D_m$$
$$= 1.6 \times 10^{-10}\,\text{m}^2\,\text{s}^{-1} \text{ with } d = 46 \times 10^{-6}\,\text{m}$$

Later, the diffusion coefficients of hexacyanoferrate(III) and hexacyanoferrate(II) were taken as equal.

5.2. *Model*

The model was run with the values of the physicochemical parameters gathered in Table 1. The thickness (δ) of the reaction layer, which lies between the dialysis membrane and the working electrode, was the only parameter difficult to determine experimentally. Its value was at least 0.5 mm because the thickness of the working electrode grid was around 0.5 mm. This thickness should be numerically adjusted by a trial and error procedure.

Figure 2 gives the theoretical current–potential curves obtained by cyclic voltammetry for a solution of 0.1 M phosphate buffer pH 7.0 containing 10 mM hexacyanoferrate(III) with a potential scan rate of 100 mV s^{-1}. Two numbers of space steps (50 and 150) were used to discretise the reaction layer. The values obtained with 50 steps were very different from those obtained with 150 steps for a thickness of 1.5 mm. However, over 150 steps, the curves were no longer modified. The differences obtained with 50 steps can be explained by observing the concentration profiles of the reduced species in solution and in the membrane (Figure 3) for a potential of 0.2 V vs SCE (indicated in Figure 2). The concentration profiles obtained with 50 or 150 steps are strictly superimposed. The method showed good convergence whatever the number of steps. Actually, the current was calculated according to Equation 11, which is proportional to the value of the ratio:

$$\frac{C_{red}^2 - C_{red}^1}{\Delta x} \tag{15}$$

where C_{red}^2 and C_{red}^1 are the values of the concentration at the first space step and on the electrode surface, respectively, and Δx is the value of the space step ($\Delta x = 10$ μm for 150 steps, and $\Delta x = 30$ μm for 50 steps). Figure 3 shows that this slope differed according to the number of steps, even if the general concentration profiles were identical. Consequently, the difference observed between the current–potential curves (Figure 2) was not ascribable to numerical divergence, but

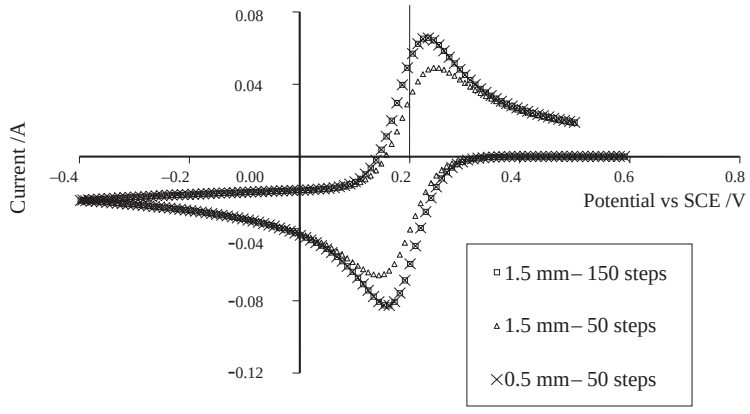

Fig. 2. Theoretical potential–current curves at 100 mV s^{-1}. Influence of the thickness of the reaction layer (δ) and of the number of steps.

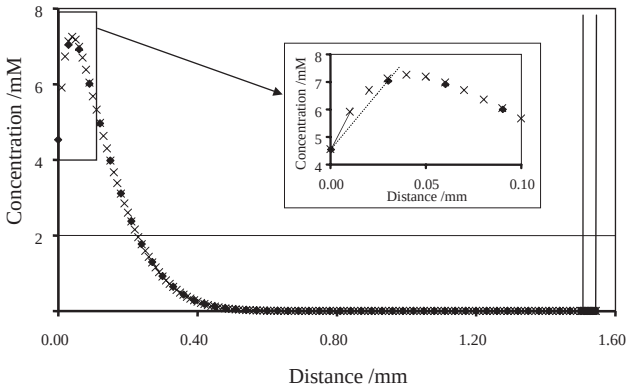

Fig. 3. Concentration profile of the reduced species as a function of the distance to the electrode at 0.2 V vs SCE for two numbers of steps: (♦) 50 steps and (×) 150 steps. Scan rate 100 mV s^{-1}; δ=1.5 mm.

only to the numerical approximation used to estimate the current. For a reaction layer thickness of 1.5 mm, 150 steps were needed to obtain correct theoretical results. To determine the influence of the reaction layer thickness (δ) and to avoid any numerical bias, we compared the curves obtained with the same value of the space step Δx. At 100 mV s^{-1}, the curves corresponding to 1.5 mm (150 steps) and 0.5 mm (50 steps) are superimposed (Figure 2); Figure 3 illustrates why the current–potential curves were not sensitive to the thickness values (0.5 and 1.5 mm). The electrochemical oxidation or reduction modified the reduced and oxidized species concentration only in a very thin diffusion

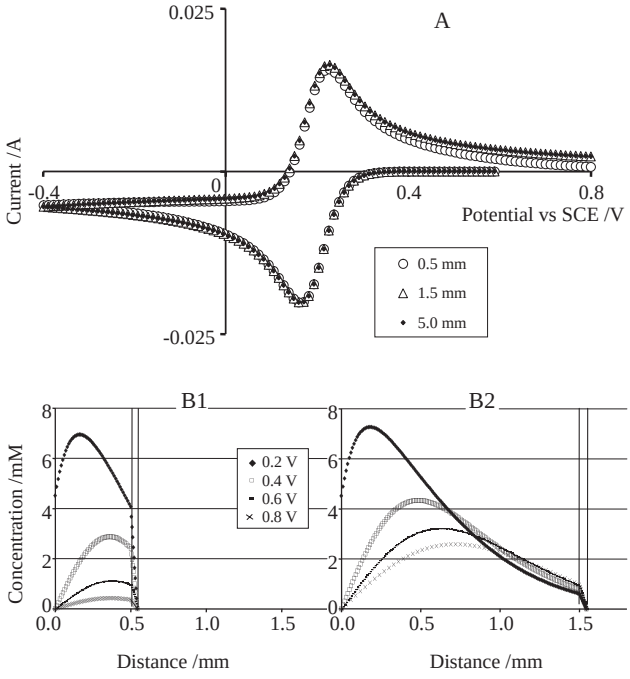

Fig. 4. (A) Current–potential curves for different values of the thickness of the reaction layer (δ). (B) Concentration profiles of the reduced form for different oxidation potentials (0.2, 0.4, 0.6 and 0.8 V vs SCE) and for two values of δ: (B1) $\delta = 0.5$ mm and (B2) $\delta = 1.5$ mm. Scan rate 5 mV s^{-1}. Initial concentration of the oxidized species: 10 mM.

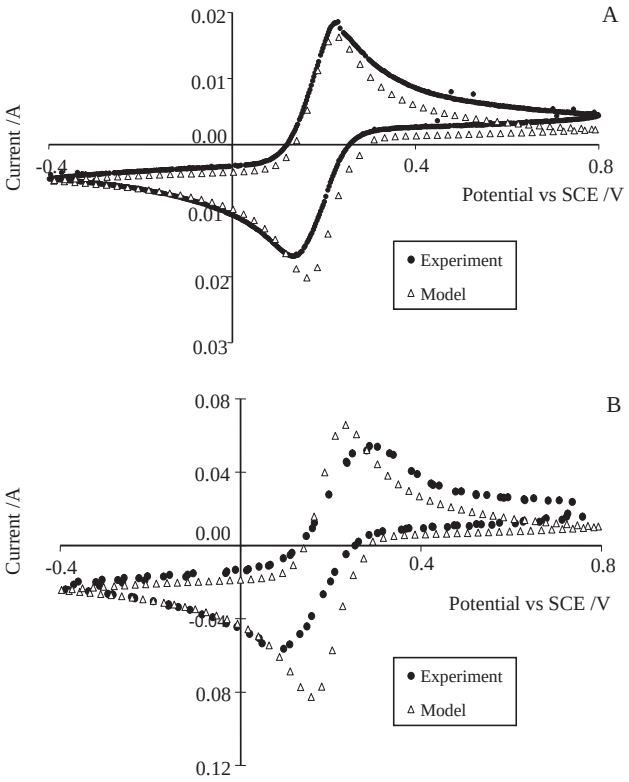

Fig. 5. Comparison between theoretical and experimental current–potential curves. Scan rate: (A) 5 mV s^{-1} and (B) 100 mV s^{-1}. Initial concentration of oxidized species: 10 mM. Parameter values were those gathered in Table 1 and δ was 1.5 mm.

layer (below 0.45 mm) inside the reaction layer. At 100 mV s^{-1}, the modifications of concentration imposed by the electrode did not extend up to the membrane. The model shows that at this scan rate (100 mV s^{-1}), δ cannot be derived from the analysis of the cyclic voltammograms.

For a scan rate of 5 mV s^{-1}, only a small influence of δ was observed for potentials over 0.4 V (Figure 4A). The concentration profiles of the reduced species were plotted at four potentials 0.2 V, 0.4 V, 0.6 V and 0.8 V and for thicknesses of 0.5 (Figure 4B1) and 1.5 mm (Figure 4B2). For a potential of 0.2 V, δ hardly affected the concentration profile near the electrode. Therefore, the electrode detected no influence of δ. For potentials greater than 0.4 V, the profiles are different, even near the electrode, according to the value of δ. The currents were consequently different. This part of the current–potential curves could be used to determine the thickness of the reaction layer. However, this scan rate does not allow estimation of the thickness if it is greater than 1.5 mm. Indeed Figure 5B shows that the position of the membrane modified the concentration profile for thicknesses lower than 1.5 mm, but for higher thicknesses, the profile and the current were not modified. This was confirmed by the curve plotted for a thickness of 5 mm (Figure 4A).

The experimental and theoretical current–potential curves were compared for two scan rates: 5 and 100 mV s^{-1} in Figure 5A and B, respectively, without

numerical adjustment of the parameter values that were given in Table 1. The flow rate in the loop was increased until it no longer effected the voltammograms. At this point the well-stirred hypothesis for Equations 5 and 6 was assumed to be valid. A satisfactory agreement between model and experiment was observed mainly for the curves obtained at 5 mV s^{-1}. Whatever the scan rate, the theoretical diffusion-limited current obtained during the oxidation scan was smaller than that obtained during the reduction scan. As the solution was considered to initially contain only oxidized species, the current obtained at the end of the reduction scan was consequently a real diffusion-limited current (at −0.4 V vs SCE). On the contrary, during the oxidation scan, only the reduced species formed during the previous reduction was oxidized. There was no supply of reduced species from the bulk. Consequently the current obtained at the end of the oxidation scan did not correspond to a diffusion-limited current but was controlled by the quantity of reduced species formed during the previous reduction scan. Consumption of the reduced species during the oxidation scan can be observed on the concentration profiles of the reduced species plotted in Figure 4B.

The few differences observed between the theoretical and the experimental curves can be explained by:

(i) Possible pollution of the hexacyanoferrate(III) solution by the reduced form. The largest difference appeared at the most anodic potentials, as if there was a small concentration of reduced species in the bulk solution. This could also explain the experimental reduction peak being slightly lower than the theoretical peak.

(ii) The most significant discrepancy was observed in the curves plotted at 100 mV s^{-1}. In this case, the deformation of the peaks is clearly characteristic of the ohmic drop effect [27]. This type of deformation is logically more visible for the faster scan rates because the current values are higher (at 0.3 V vs SCE: 0.06 A for 100 mV s^{-1} instead of 0.02 A for 5 mV s^{-1}). A rather high ohmic drop may be explained by the position of the reference electrode, which is separated from the working electrode by the dialysis membrane.

(iii) Finally, the difference between the theoretical representation of the electrode and its physical reality must be evoked. Actually, the electrode was a three-dimensional platinum grid, but it was only considered in the model as an ideal plane surface located at $x = 0$. This discrepancy might also introduce some bias in the model.

Despite these few differences, the theoretical model combined with the preliminary experiments gave a good description of the reactor behaviour. The good match between theoretical and experimental data also show that each technical problem that was initially encountered was solved correctly: the potential of the working electrode was well controlled, the whole surface area of the electrode was uniformly accessible by the substrate, and the substrate diffuses through the whole surface area of the membrane. Problems linked to air bubbles no longer occurred during the filling of the reaction layer via the capillary. All these problems were not noted above, because they did not have great intrinsic interest. Nevertheless, each of these factors would result in a significant discrepancy between model and experiment. The model is consequently a useful tool for failure diagnosis, and should be useful for further reactor scale-up.

5.3. *Enzyme-catalysed synthesis*

The final design of the D-MER was used to carry out the GOD catalysed oxidation of glucose. The phosphate buffer pH 7.0 circulating in the working loop (44 cm^3 total volume) initially contained 0.25 M glucose. The potential of the working electrode was maintained at 0.45 V vs SCE, and 112 units GOD were introduced into the reaction layer by the capillary (noted (16) on Figure 1). The solution was continuously aerated by air bubbles in the storage tank. The GOD catalysed reaction (Reaction 1) occurred in the reaction layer of the D-MER only. This reaction resulted in glucose consumption and hydrogen peroxide production. The immediate consumption of hydrogen peroxide on the electrode surface (Reaction 2) protected the enzyme against drastic inhibition. The evolution of glucose concentration in the storage tank is reported in Figure 6. More than 25% of the initial glucose concentration was consumed after three hours electrolysis. A control experiment was carried out in a simple beaker containing 43 cm^3 phosphate buffer solution (0.1 M, pH 7.0) with 0.29 mM glucose and 100 U GOD. No electrochemical process was applied in this experiment. Glucose concentration evolution is also reported in Figure 6. After three hours only 4% of the initial glucose amount was transformed. In this case hydrogen peroxide produced by the reaction significantly inhibited the enzyme. It should be noted that in the field of biochemistry, and particularly in glucose biosensor

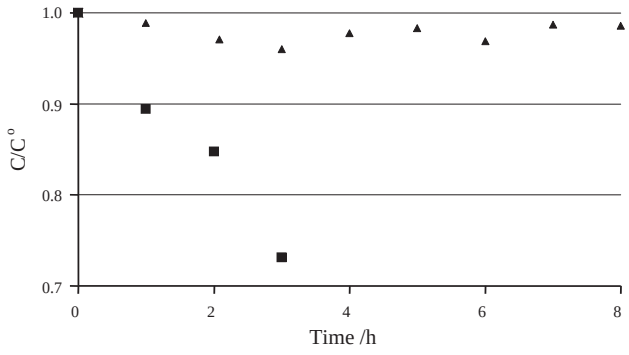

Fig. 6. Dimensionless glucose concentration as a function of time obtained: (■) in the D-MER. Initial glucose concentration 0.25 M, GOD activity 112 U, in phosphate buffer solution 0.1 M pH 7.0, volume 44 cm^3; (▲) in a beaker without electrochemical process. Initial glucose concentration 0.29 M, GOD activity 100 U, in phosphate buffer solution 0.1 M pH 7.0, volume 43 cm^3.

design, this reaction is generally used with lower initial glucose concentrations, where inhibition phenomena are less evident. This preliminary experiment revealed the real efficiency of the D-MER. In the case of glucose oxidation catalysed by GOD, use of this reactor makes it possible to increase the concentration of substrate, and this may provide new interest in this reaction for gluconic acid production.

6. Conclusion

The D-MER designed for enzymatic synthesis was investigated with a simple electrochemical reaction. A model was developed to fit the voltammetry experiments based on the description of the coupled phenomena: electrochemical reaction/mass transfer in the reaction layer/mass transfer in the membrane. The good agreement of theoretical results and experimental data showed that the proposed D-MER design can efficiently process enzymatic reactions, as demonstrated by the GOD-catalysed oxidation of glucose. Work is in progress to optimise this reaction [28], and also to perform the reduction of ketone compounds catalysed by NAD-dependent alcohol dehydrogenase [29].

References

1. R. Devaux-Basseguy, P. Gros and A. Bergel, *J. Chem. Tech. Biotechnol.* **68** (1997) 389.
2. A. Pollak, H. Blumenfeld, M. Wax, R.L. Baughn and G.M. Whitesides, *J. Am. Chem. Soc.* **102** (1980) 6324.
3. R. DiCosimo, C.-H. Wong, L. Daniels and G.M. Whitesides, *J. Org. Chem.* **46** (1981) 4622.
4. H. Maeda and S. Kajiwara, *Biotechnol. Bioeng.* **27** (1985) 596.
5. C. Bourdillon, J.M. Laval and D. Thomas, *J. Electrochem. Soc.* **133** (1986) 706.
6. S.B. Sobolov, M.D. Leonide, A. Bartosko-Malik, K.I. Voivodov, F. McKinney, J. Kim and A.J. Fry, *J. Org. Chem.* **61** (1996) 2125.
7. O. Miyawaki and T. Yano, *Enz. Microb. Technol.* **15** (1993) 525.
8. P.N. Bartlett, D. Pletcher and J. Zeng, *J. Electrochem. Soc.* **144** (1997) 3705.
9. M.D. Benardski, H.K. Chenault, E.S. Simon and G.M. Whitesides, *J. Am. Chem. Soc.* **109** (1987) 1283.
10. M.R. Kula and C. Wandrey, *Methods Enzymol.* **136** (1987) 9.
11. K. Seelbach and U. Kragl, *Enz. Microb. Technol.* **20** (1997) 389.
12. S. Kise and M. Hayashida, *J. Biotechnol.* **14** (1990) 221.
13. M. Howaldt, A. Gottlob, K.D. Kulbe and H. Chmiel, *Ann. N.Y. Acad. Sci.* **542** (1988) 400.
14. M. Ikemi, N. Koizumi and Y. Ishimatsu, *Biotechnol. Bioeng.* **36** (1990) 149.
15. R.W. Coughlin, M. Aizawa, B.F. Alexander and M. Charles, *Biotechnol. Bioeng.* **17** (1975) 515.
16. B. Brielbeck, M. Frede and E. Steckhan, *Biocatalysis* **10** (1994) 49.
17. D. Hekmat, J. Danninger, H. Simon and D. Vortmeyer, *Enz. Microb. Technol.* **24** (1999) 471.
18. A. Bergel and M. Comtat, *Biotechnol. Bioeng.* **28** (1986) 728.
19. M.T. Grimes and D.G. Drueckhammer, *J. Org. Chem.* **58** (1993) 6148.
20. P. Buzzini, M. Gobbetti, J. Rossi and S. Haznedari, *Ann. Microbiol. Enzimol.* **43** (1993) 195.
21. N.V. Sankpal and B.D. Kulkarni, *Process Biochem.* **37** (2002) 1343.
22. J. Crank, 'The Mathematics of Diffusion' (Oxford University Press, Oxford, 1975).
23. A. Kunst, *in* H.U. Bergmeyer, J. Bergmeyer and M. Grassl (Eds), 'Methods of Enzymatic Analysis' (Verlag Chemie, Weinheim, 1984), p. 163.
24. A. Bard and L.R. Faulkner, 'Electrochemical, Methods, Fundamentals and Application' (Wiley, New York, 1980).
25. D.A. Gough and J.K. Leypoldt, *Anal. Chem.* **51** (1979) 439.
26. D.A. Gough and J.K. Leypoldt, *AIChE J.* **26** (1980) 1013.
27. A. Bergel and M. Comtat, *J. Electroanal. Chem.* **285** (1990) 11.
28. K. Délécouls-Servat, A. Bergel and R. Basséguy, Bioprocess and Biosystems Engineering (2003), submitted.
29. K. Délécouls-Servat, R. Basséguy and A. Bergel, *Chem. Eng. Sci.* **57** (2002) 4633.